Title

Studying squark mass spectrum through gluino decay at 100 TeV future hadron colliders

Authors

Chigusa, So

Hamaguchi, Koichi

Moroi, Takeo

et al.

Publication Date

2021-06-01

DOI

10.1016/j.physletb.2021.136332

Peer reviewed

KEK-TH-2298
IPMU21-0012
February, 2021

Studying squark mass spectrum through gluino decay at 100 TeV future hadron colliders

So Chigusa[a,b,c], Koichi Hamaguchi[d,e], Takeo Moroi[d,e], Atsuya Niki[d], and Kosaku Ono[d]

[a] *Berkeley Center for Theoretical Physics, Department of Physics, University of California, Berkeley, CA 94720, USA*

[b] *Theoretical Physics Group, Lawrence Berkeley National Laboratory, Berkeley, CA 94720, USA*

[c] *KEK Theory Center, IPNS, KEK, Tsukuba, Ibaraki 305-0801, Japan*

[d] *Department of Physics, University of Tokyo, Tokyo 113-0033, Japan*

[e] *Kavli IPMU (WPI), UTIAS, University of Tokyo, Kashiwa, Chiba 277-8583, Japan*

Abstract

We study the prospect of determining the decay properties of the gluino in the supersymmetric (SUSY) standard model at a 100 TeV future hadron collider. We consider the case where the neutral Wino is the lightest superparticle. In this case, the long-lived charged Wino can be used to eliminate standard model backgrounds, which enables us to study the details of superparticles. We show that, based on the analysis of the numbers of high p_T leptons, boosted W-jets, and b-tagged jets, we may determine the gaugino species and the quark flavors in the gluino decay. With such determinations, we can obtain information about the mass spectrum of squarks even if squarks are out of the kinematical reach.

1 Introduction

Collider experiments at the energy frontier are important in understanding the properties of elementary particles. In the last decade, the Large Hadron Collider (LHC) has not only discovered the Higgs boson [1, 2] but also has revealed its properties. The results from the LHC experiment (as well as those from other experiments) have been essential to confirm the validity of the standard model (SM) as the effective theory for the energy scale below the TeV scale. Despite the success of the SM, however, it is widely believed that the SM is not the ultimate theory and that there should show up physics beyond the SM (BSM). This is because there are still mysteries that cannot be explained in the framework of the SM; for example, from the particle physics point of view, the charge quantization (which is naturally explained in the grand unified theory (GUT)) cannot be explained in the standard model, and from cosmology point of view, the origin of dark matter is not understood.

One of the tasks of the future energy frontier experiments is to find signals of BSM physics and to study its properties. In the next decade, the LHC Run-3/HL-LHC will play such a role and will try to discover BSM particles. However, the searches are limited by the collider energy and the discovery is impossible if the BSM particles are out of the kinematical reach. For example, in the supersymmetric (SUSY) SM with the Wino lightest superparticle (LSP), the thermal Wino can become dark matter if its mass is about 2.9 TeV and hence such a model is well motivated. However, such a heavy Wino is out of the reach of the LHC experiment [3]. For the discovery and the study of the BSM particles, we may need a collider with the center of mass energy much higher than the LHC.

Recently, the possibilities of such high energy colliders have been discussed. In this paper, we consider circular pp collider with the center of mass energy of about 100 TeV, i.e., future circular collider (or dubbed as FCC-hh). FCC-hh is a prominent candidate for a future energy frontier experiment [4].

Here, we discuss the prospect of studying the properties of superparticles in SUSY SM at the FCC-hh. We will pay particular attention to the so-called pure gravity mediation model of SUSY breaking [5, 6, 7] based on anomaly mediation [8, 9]; such a model naturally results in the Wino LSP (possibly with the Wino mass of $\sim 2.9\,\text{TeV}$) so that the Wino can be a viable dark matter candidate. In addition, with the introduction of SUSY particles, the gauge coupling unification at the GUT scale of about $10^{16}\,\text{GeV}$ is suggested. Thus, even though the signal of SUSY has not been discovered yet, it is still an attractive candidate for the BSM physics. It is important to understand what we can learn about such a model at the FCC-hh. Indeed, there have been efforts to investigate the potential of the FCC-hh for the study of the pure gravity mediation SUSY model. It has been discussed that the FCC-hh will discover the Wino LSP using the fact that the decay length of the charged Wino may become macroscopic [3]. It has also been pointed out that the mass spectrum of the gauginos and the lifetime of the charged Wino can be studied at the FCC-hh after the discovery of the Wino LSP [10, 11].

In this paper, a possibility to study the decay properties of the gluino $\tilde{g}$ at the FCC-hh is discussed. (For related studies at the LHC, see [12, 13].) In the pure gravity mediation

model, the gluino decays into a quark anti-quark pair and a Wino $\tilde{W}$ or a Bino $\tilde{B}$. We will show that, by analyzing the numbers of high p_T leptons, boosted W-jets, and b-tagged jets in the gluino production events, the gaugino species and the quark flavors in the gluino decay may be understood. As the partial branching ratios of the gluino are model dependent and sensitive to the squark masses, the detailed study of the gluino decay may give information about the mass spectrum of squarks which may be out of the kinematical reach of the FCC-hh.

The organization of this paper is as follows. In Section 2, we introduce our representative model based on which we perform the Monte Carlo (MC) analysis. In Section 3, we explain the detail of our MC analysis and show the numerical results. In Section 4, we discuss implications of the determination of the partial branching ratios of the gluino at the FCC-hh. The results are summarized in Section 5.

2 Model

We first introduce the SUSY model of our interest. As we have mentioned, we consider the pure gravity mediation model in which the gaugino masses are from the effect of anomaly mediation while the SUSY breaking scalar mass squared parameters originate from the supergravity effect. In such a framework, the scalar masses and the Higgsino mass μ are of the order of the gravitino mass $m_{3/2}$ while the gaugino masses are one-loop suppressed relative to the scalar masses. The model has several phenomenological advantages. First, the SM-like Higgs mass can be pushed up to the observed value of $\sim 125\,\mathrm{GeV}$ [14] by radiative corrections [15, 16, 17]. Second, the heavy sfermion masses suppress the CP and flavor violating processes mediated by SUSY particles in the loop, which significantly relaxes the SUSY CP and flavor problems. (See, however, [18, 19].) Furthermore, cosmologically, the neutral Wino can be a viable candidate of dark matter; in particular, if the Wino mass is $\sim 2.9\,\mathrm{TeV}$, the thermal relic abundance of Wino becomes consistent with the present dark matter density [20]. Motivated by these, in the following, we consider the pure gravity mediation model with gaugino masses of $O(1)\,\mathrm{TeV}$ and the gravitino mass of $O(10-100)$ TeV.

In such a model, at the FCC-hh with the center-of-mass energy of $\sim 100\,\mathrm{TeV}$, the gauginos are the primary targets while the sfermions may be hardly produced. Hereafter, we consider the case where the gauginos are accessible with the FCC-hh while the sfermions are out of the kinematical reach. For our numerical analysis in the next section, we adopt the mass spectrum of the gauginos suggested by the model of pure gravity mediation; the sample points adopted in our analysis are summarized in Table 1, in which the Bino, Wino, and gluino masses (denoted as $m_{\tilde{B}}$, $m_{\tilde{W}}$, and $m_{\tilde{g}}$, respectively), as well as the gluino pair production cross section for $\sqrt{s} = 100$ TeV, are shown. We assume that the Wino is the LSP with a mass of 2.9 TeV. For more details of the sample points, see Ref. [10].

In discussing the collider phenomenology of the model of our interest, one remarkable feature is the property of the Wino LSP. Because the Wino is in the adjoint representation of $SU(2)_L$, there exist neutral and charged Winos, $\tilde{W}^0$ and $\tilde{W}^\pm$, respectively. Without the

	Point 1	Point 2
$m_{\tilde{B}}$ [GeV]	3660	4060
$m_{\tilde{W}}$ [GeV]	2900	2900
$m_{\tilde{g}}$ [GeV]	6000	7000
$\sigma(pp \to \tilde{g}\tilde{g})$ [fb]	12.5	4.4

Table 1: Gaugino masses and gluino pair production cross section (for the center-of-mass energy of 100 TeV) for the Sample Points 1 and 2. We use the NLO + NLL gluino production cross section given in [21, 4].

effects of the electroweak symmetry breaking the masses of neutral and charged Winos are degenerate. The electroweak symmetry breaking generates a small mass gap between the neutral and charged Winos through a loop effect and the charged Winos dominantly decay as $\tilde{W}^{\pm} \to \tilde{W}^0 \pi^{\pm}$. Because of the high mass degeneracy, the lifetime of the charged Wino becomes significantly long; the most precise calculation gives [22]

$$c\tau \simeq 5.75\,\mathrm{cm}, \tag{2.1}$$

where τ is the lifetime while c is the speed of light. When $\mu \gg m_{\tilde{W}} \gg m_W$, the lifetime is almost independent of the Wino mass. Then, once produced at the FCC, the charged Wino may fly a macroscopic length of $O(1-10)\,\mathrm{cm}$. Such a long-lived charged Wino may be identified if it goes through several layers of the inner pixel detector of the FCC-hh, and it can be regarded as a characteristic feature of the SUSY signal. As we will discuss in the next section, the long-lived charged Wino can be used to remove the SM background.

The subject of this paper is to discuss the possibility of studying the decay properties of the gluino at the FCC-hh. Here, for simplicity, we consider the case where the flavor violating decay of the gluino is negligible. Then, the partial decay rates of the gluino are given by [23, 24, 13][#1]

$$\Gamma(\tilde{g} \to \tilde{B} u_{Li} \bar{u}_{Li}) = \Gamma(\tilde{g} \to \tilde{B} d_{Li} \bar{d}_{Li}) = \frac{1}{1536\pi^3} \frac{g_s^2 g'^2}{36} \frac{m_{\tilde{g}}^5}{m_{\tilde{Q}_i}^4} f\left(\frac{m_{\tilde{B}}}{m_{\tilde{g}}}\right), \tag{2.2}$$

$$\Gamma(\tilde{g} \to \tilde{B} u_{Ri} \bar{u}_{Ri}) = \frac{1}{1536\pi^3} \frac{4 g_s^2 g'^2}{9} \frac{m_{\tilde{g}}^5}{m_{\tilde{u}_i}^4} f\left(\frac{m_{\tilde{B}}}{m_{\tilde{g}}}\right), \tag{2.3}$$

$$\Gamma(\tilde{g} \to \tilde{B} d_{Ri} \bar{d}_{Ri}) = \frac{1}{1536\pi^3} \frac{g_s^2 g'^2}{9} \frac{m_{\tilde{g}}^5}{m_{\tilde{d}_i}^4} f\left(\frac{m_{\tilde{B}}}{m_{\tilde{g}}}\right), \tag{2.4}$$

[#1] Here, we neglect the renormalization group effect on the partial decay rates. At the one-loop level, the effects of the strong gauge coupling constant, which are the most important, are universal to all the final-state quark flavors and does not affect our later discussion about the study of the ratios of squark masses. In addition, the effects of the top Yukawa interaction, which is relevant only for the processes with third generation quarks in the final state, is of $O(1)$ % for the parameter region we consider. (See, for example, [13].) We also neglect the effects of the left-right mixing and the two-body decay $\tilde{g} \to \tilde{B} g$ (with g being gluon), which are unimportant for the case of our study [24].

$$\Gamma(\tilde{g} \to \tilde{W}^0 u_{Li} \bar{u}_{Li}) = \Gamma(\tilde{g} \to \tilde{W}^0 d_{Li} \bar{d}_{Li}) = \frac{1}{1536\pi^3} \frac{g_s^2 g^2}{4} \frac{m_{\tilde{g}}^5}{m_{\tilde{Q}_i}^4} f\left(\frac{m_{\tilde{W}}}{m_{\tilde{g}}}\right), \tag{2.5}$$

$$\Gamma(\tilde{g} \to \tilde{W}^- u_{Li} \bar{d}_{Li}) = \Gamma(\tilde{g} \to \tilde{W}^+ d_{Li} \bar{u}_{Li}) = \frac{2}{1536\pi^3} \frac{g_s^2 g^2}{4} \frac{m_{\tilde{g}}^5}{m_{\tilde{Q}_i}^4} f\left(\frac{m_{\tilde{W}}}{m_{\tilde{g}}}\right), \tag{2.6}$$

where $i = 1 - 3$ denotes generation index, and

$$\begin{aligned} f(x) =& 1 - 8|x|^2 - 12|x|^4 \ln|x|^2 + 8|x|^6 - |x|^8 \\ &+ 2(1 + 9|x|^2 + 6|x|^2 \ln|x|^2 - 9|x|^4 + 6|x|^4 \ln|x|^2 - |x|^6)\mathrm{Re}(x). \end{aligned} \tag{2.7}$$

Because we are interested in the case where the gluino mass is much larger than the quark masses, we neglect the quark masses. As one can see, the partial decay rates are sensitive to the mass spectrum of squarks and are highly model dependent. Thus, with the detailed studies of branching ratios of the gluino, we can obtain information about the mass spectrum of squarks.

In the sample points we adopted, the Bino is unstable and decays into a charged or neutral Wino. In the limit of $\mu \gg m_{\tilde{B}/\tilde{W}} \gg m_W$, the partial decay rates of the dominant decay processes of the Bino are insensitive to the sfermion masses, and the Bino dominantly decays into $\tilde{W}^\pm W^\mp$ or $\tilde{W}^0 h$ with the branching fractions given as follows [10]:

$$\mathrm{Br}(\tilde{B} \to \tilde{W}^+ W^-) = \mathrm{Br}(\tilde{B} \to \tilde{W}^- W^+) \simeq \mathrm{Br}(\tilde{B} \to \tilde{W}^0 h) \simeq \frac{1}{3}. \tag{2.8}$$

The decay process $\tilde{B} \to \tilde{W}^0 Z$ is subdominant when μ is much larger than $m_{\tilde{B}}$ and $m_{\tilde{W}}$.

3 Analysis

3.1 Setup

In this section, we discuss the measurement of the branching ratios of the gluino decay at a 100 TeV collider. We utilize the signal events due to the pair production of the gluino:

$$pp \to \tilde{g}\tilde{g}, \tag{3.1}$$

followed by the decay of each gluino with a charged Wino in the final state:

$$\tilde{g} \to \begin{cases} \tilde{B} q \bar{q}, \text{ with } \tilde{B} \to \tilde{W}^\pm W^\mp, \\ \tilde{W}^\pm q \bar{q}. \end{cases} \tag{3.2}$$

We note that the gluino and the Bino may also decay into neutral Wino (and SM particles); the branching ratios of the gluino and Bino are determined with these decay modes in our simulation. However, events with such decay processes do not contribute to the signal, as we discuss below. As discussed in [3], for the sample points we have adopted, the Wino is within

the discovery reach of the FCC-hh using a disappearing track signature. After the discovery of the gauginos, all the gaugino masses can be measured at the FCC-hh [10]. In addition, the lifetime of charged Wino can be determined by analyzing the distribution of the flight length [11]. Thus, in the following analysis, we assume that we can use the information about the gaugino masses and the Wino lifetime and discuss how and how well we can determine the branching ratios of the gluino decay processes. In particular, the information about the gluino mass is essential to predict the production cross section of the gluino pair, while the Wino lifetime is necessary to determine the detection rate of the long-lived charged Wino at the inner pixel detector (see discussion below). In principle, the cross section for the process $pp \to \tilde{g}\tilde{g}$, as well as the survival detection probability of the charged Wino, can be theoretically calculated once the gaugino masses and the Wino lifetime are known. In our analysis, we assume that reliable calculations of these quantities are possible at the time of the FCC-hh experiment. We neglect systematic uncertainties in our MC analysis and comment on them at the end of this section.

As shown in Eqs. (2.2) – (2.6), $\mathrm{Br}(\tilde{g} \to \tilde{W} q\bar{q})$ becomes large (small) when the left-handed squarks are light (heavy) compared to the right-handed ones. Moreover, when the third generation squarks are light (heavy), the branching ratios into the third generation quarks become enhanced (suppressed). Motivated by these features, we study how well we can constrain (i) the probability that the gluino decays into a Bino, not a Wino (which we call x), and (ii) the probability that the gluino decays into the third generation quark anti-quark pair rather than the first or second generation one (which we call y):

$$\sum_{q} \mathrm{Br}(\tilde{g} \to \tilde{B} q\bar{q}) = x, \tag{3.3}$$

$$\sum_{q,q'} \mathrm{Br}(\tilde{g} \to \tilde{W} q\bar{q}') = 1 - x, \tag{3.4}$$

$$\sum_{q,q'=t,b} \Big[\mathrm{Br}(\tilde{g} \to \tilde{B} q\bar{q}) + \mathrm{Br}(\tilde{g} \to \tilde{W} q\bar{q}')\Big] = y, \tag{3.5}$$

$$\sum_{q,q'=u,d,c,s} \Big[\mathrm{Br}(\tilde{g} \to \tilde{B} q\bar{q}) + \mathrm{Br}(\tilde{g} \to \tilde{W} q\bar{q}')\Big] = 1 - y. \tag{3.6}$$

Thus, in our analysis, a model point is characterized by a set of (x, y) as well as gaugino masses. More concretely, in our Monte Carlo simulation, the gluino branching ratios are set as follows:[#2]

$$\mathrm{Br}(\tilde{g} \to \tilde{B} q\bar{q}) = \begin{cases} \frac{1}{4}x(1-y) & (q = u, d, c, s) \\ \frac{1}{2}xy & (q = t, b) \end{cases}, \tag{3.7}$$

$$\mathrm{Br}(\tilde{g} \to \tilde{W}^0 q\bar{q}) = \begin{cases} \frac{1}{12}(1-x)(1-y) & (q = u, d, c, s) \\ \frac{1}{6}(1-x)y & (q = t, b) \end{cases}, \tag{3.8}$$

[#2]In order to realize Eqs. (3.7) – (3.9), we assume several relations among squark masses: (i) masses of 1st and 2nd generation left-handed squarks are degenerate, (ii) the ratio $m_{\tilde{u}_i}/m_{\tilde{d}_i} = \sqrt{2}$ for all the generations, and (iii) $m_{\tilde{Q}_3}/m_{\tilde{Q}_{1,2}} = m_{\tilde{u}_3}/m_{\tilde{u}_{1,2}} = m_{\tilde{d}_3}/m_{\tilde{d}_{1,2}}$ (see Eqs. (2.2) – (2.6)).

$$\mathrm{Br}(\tilde{g} \to \tilde{W}^- q\bar{q}') = \mathrm{Br}(\tilde{g} \to \tilde{W}^+ q'\bar{q}) = \begin{cases} \frac{1}{6}(1-x)(1-y) & (q\bar{q}' = u\bar{d}, c\bar{s}) \\ \frac{1}{3}(1-x)y & (q\bar{q}' = t\bar{b}) \end{cases} . \tag{3.9}$$

Flavor violating decay processes of the gluino are assumed to be negligible. For larger (smaller) x, the numbers of leptons and boosted W-jets increase (decrease) because they are produced by the decay of the Bino. (Notice that high p_T leptons are produced by the decay of W bosons from the Bino decays.) In addition, larger y is expected to enhance the number of b-tagged jets. The parameter space in our analysis is thus $0 \leq x, y \leq 1$ and we study how well we can determine the x and y parameters at the FCC-hh using these features in the following.

We comment that, in general, the partial branching ratios cannot be determined just by x and y, and that Eqs. (3.7) – (3.9) are examples which realize Eqs. (3.3) – (3.6). As we will see below, the accuracy of the x determination is insensitive to the quark flavors from the gluino decay (i.e., the choice of y) while that of the y determination does not depend so much on the gaugino species (i.e., the choice of x). Thus, we expect that our main conclusions are not significantly altered by the detail of the partial branching ratios for a given set of (x, y).

3.2 Method

In the sample points we take, the gluino is within the kinematical reach of the FCC, and the gluino pair is produced as $pp \to \tilde{g}\tilde{g}$. If signals are selected only using a missing E_T cut, a significant amount of SM backgrounds are expected. In order to eliminate the SM backgrounds, we use the fact that the signal on inner pixel detectors given by charged Winos can be used to identify the SUSY events. As we have mentioned, the decay length of the charged Wino can be as long as ~ 10 cm. Such a long-lived charged Wino hits several layers of the inner pixel detector and, after the decay, it does not leave any energetic activity in outer detectors. Then, the long-lived charged Wino is regarded as a short high p_T track, which is hardly mimicked by SM events. Thus, by requiring long-lived charged Wino tracks, a significant reduction of the SM backgrounds is expected.

In our analysis, we impose the following requirements on the signal events:

1. The missing transverse energy E_T is larger than 1 TeV.

2. Each gluino has charged Wino in its decay chain; each charged Wino is assumed to be identified by the inner pixel detector with imposing the following requirements 3 and 4.

3. The pseudorapidities η of both charged Winos are smaller than 1.5.

4. The transverse flight lengths L_T of both charged Winos should be longer than 10 cm. (Here, we assume that the transverse distance to the fourth layer of the pixel detector is 10 cm so that each charged Wino goes through four layers of the pixel detector.)

We assume that the SM backgrounds become negligible after imposing these requirements [3, 10].

By using the information from the signal events, we can determine the partial decay rate of the gluino as we discuss in detail in the following. For each event, we count the numbers of leptons ($e^{\pm}$ and $\mu^{\pm}$), boosted W-jets, and b-tagged jets:

- We use leptons and b-tagged jets whose transverse momenta are larger than 200 GeV.
- We define the "boosted W-jets" as jets with mass 60 GeV $< m_{jet} <$ 100 GeV, the ratio of N-subjettiness [25] $\tau_2/\tau_1 < 0.3$ [26], and $p_T > 200$ GeV.

In order to investigate how well we can constrain the x and y parameters, we perform an MC analysis. The flowchart of our MC simulation is shown in Fig. 1. We use `MadGraph5_aMC@NLO 2.7.2` [27, 28] to generate $pp \to \tilde{g}\tilde{g}$ events. The effect of the initial state radiation is not included. Decay and hadronization processes are simulated by using `PYTHIA8` [29]. Detector simulation is done by `Delphes 3.4.2` [30] using `FCChh.tcl` card. The `MSTW2008lo68cl_nf3` parton distribution function is used [31].

The disappearing track of charged Winos cannot be simulated by `Delphes` by default; charged Winos are treated in a similar way as other charged particles in `Delphes`. In order to simulate the decay and the detection of charged Winos, we calculate the flight-length distribution of each charged Wino using the information provided by `hepmc` file (which is the output of `PYTHIA8`), while each charged Wino is treated as non-detectable neutral particles in `Delphes`. (In the `Delphes` simulation, we use the `hepmc` file in which the particle ID number of charged Wino is changed to that of neutral Wino.)

Combining the output of `Delphes` simulation and the flight-length distributions of charged Winos, we calculate the distributions of the number of leptons, boosted W-jets, and b-tagged jets. The analysis is performed by using `ROOT 6.18` [32].

Now we explain how we study the prospects of constraining x and y parameters at the FCC-hh. In our analysis, the parameter space is discretized as $x, y \in [0.0, 0.1, 0.2, ..., 1.0]$. We determine the partial branching ratios of the gluino for given x and y (see Eqs. (3.7) – (3.9)). Then, for each set of (x, y), we simulate $pp \to \tilde{g}\tilde{g}$ process and choose signal events satisfying the requirements 1 – 4 introduced before. An example of the cut flow, taking $x = 0.5$ and $y = 0.5$, is shown in Table 2. Then, using the signal events passing the cuts, we calculate the expected numbers of leptons, boosted W-jets, and b-tagged jets. With the distributions of these numbers on the x vs. y plane, we determine the accuracy of the determinations of x and y parameters for given values of the luminosity.

Here, we use the following classifications of the events:

- The total number of leptons ($e^{\pm}$ and $\mu^{\pm}$) is zero (L0) or non-zero (L1).
- The number of boosted W-jet is zero (W0) or non-zero (W1).
- The number of b-tagged jet is less than 2 (B01) or 2 or larger (B2).

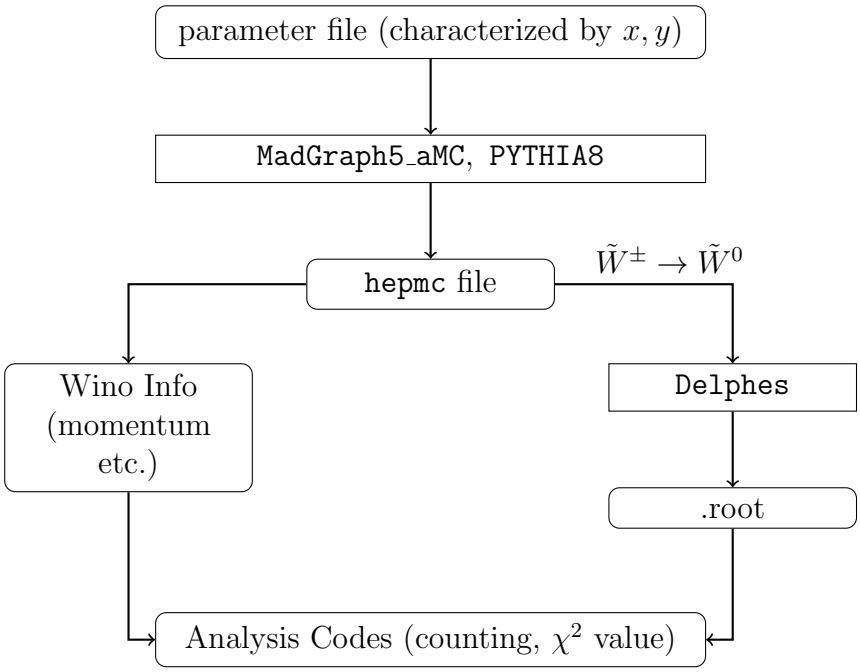

Figure 1: The flowchart of MC simulation. Rectangular means simulator and rounded corner rectangular means data file and analysis codes.

condition	number of events
total events	100000
two $\tilde{W}^{\pm}$	44341
$\eta \leq 1.5$	25300
MET: $E_T \geq 1$ TeV	19992
$L_T \geq 10$ cm	536

Table 2: The cut flow for the sample point 1 with $x = 0.5,\ y = 0.5$, using 100000 events of gluino pair production.

Based on the above classifications, we define eight signal regions characterized by (Lℓ, Ww, Bb), where $\ell = 0$ or 1, $w = 0$ or 1, and $b = 01$ or 2; all the signal events passing the requirements 1 – 4 are classified into one of eight signal regions. For a given luminosity, we calculate the expected numbers of events falling into eight signal regions (denoted as N_i with $i = 1 - 8$). In our analysis, N_i is calculated as

$$N_i = \frac{\mathcal{L}\sigma_{pp\to\tilde{g}\tilde{g}}}{N_{\rm MC}} \sum_{A=1}^{N_{\rm MC}} \delta_A^{(\rm cuts)} \delta_{(\rm L\ell,Ww,Bb)_A,(\rm L\ell,Ww,Bb)_i} P_A^{(1)} P_A^{(2)}, \tag{3.10}$$

where the summation is over all the event samples generated in the MC analysis, and $N_{\rm MC}$ is the total number of event samples (which is taken to be 100000 in our analysis). Here,

$\delta_A^{(\mathrm{cuts})}$ is 1 (0) if A-th event satisfies (does not satisfy) the kinematical requirements 1 – 3, while $\delta_{(\mathrm{L}\ell,\mathrm{W}w,\mathrm{B}b)_A,(\mathrm{L}\ell,\mathrm{W}w,\mathrm{B}b)_i}$ is 1 (0) if A-th event falls (does not fall) into i-th signal region. In addition, $P_A^{(1)}$ ($P_A^{(2)}$), which takes care of the requirement 4, is the probability that the transverse flight length of the first (second) charged Wino produced in A-th event sample is longer than $L_0 = 10$ cm.[#3]

We calculate the expected numbers of events in eight signal regions for the 11×11 different choices of (x, y); the result is denoted as $N_i^{(x,y)}$. Once the set of $N_i^{(x,y)}$ is obtained, we perform the χ^2 analysis to estimate the expected accuracy of the determination of (x, y). The difference of the χ^2 variable between one model point with (x_0, y_0), called reference point, and another with (x, y), called trial point, is given by

$$\Delta\chi^2 = \sum_i \frac{\left(N_i^{(x,y)} - N_i^{(x_0,y_0)}\right)^2}{N_i^{(x_0,y_0)}}. \tag{3.11}$$

In our analysis, this value follows χ^2 distribution with two degrees of freedom.

3.3 Numerical results

Now, we show our numerical results. Before discussing the expected accuracies in the x and y determination, let us see how the numbers of leptons, boosted W-jets, and b-tagged jets depend on x and y. In Figs. 2 and 3, we show the distribution of the number of events for the sample points 1 and 2, respectively; red, blue, and green numbers are the numbers of events categorized in L1 (with any numbers of W-jet and b-tagged jet), W1, and B2, respectively, for some choices of (x, y). In addition, we also show the total number of signal events in black. We can see that the total number of signal events decreases as x increases. This is because, for a larger value of x, the average number of final state particles becomes larger and the averaged velocity of the charged Wino becomes smaller, resulting in the suppression of the survival probability of $\tilde{W}^{\pm}$. As expected, the numbers of leptons and boosted W-jets increase as the x parameter becomes larger; this is because the leptons and boosted W-jets originate from the decay process $\tilde{B} \to \tilde{W}^{\pm} W^{\mp}$. They also depend on y because of the W boson from the top quark decay. The number of b-tagged jets shows a significant dependence on y. The number of b-tagged jets also depends slightly on x, which is mainly due to the x-dependence of the total number of signal events. Thus, we can expect that the x and y parameters can be constrained with the procedure explained in the previous subsection.

In Figs. 4 and 5, we show expected 95% C.L. constraints on the (x, y) plane for the sample points 1 and 2, respectively, taking the integrated luminosity of 1, 3, and 10 ab^{-1}.

[#3]The probability that the transverse flight length of a charged Wino is longer than L_0 is

$$P = \exp\left(\frac{-L_0}{c\tau\beta\gamma\sin\theta}\right),$$

where $c\beta$ is the velocity of the Wino, $\gamma \equiv (1-\beta^2)^{-1/2}$, and θ is the angle between the beam axis and the flight direction of the Wino.

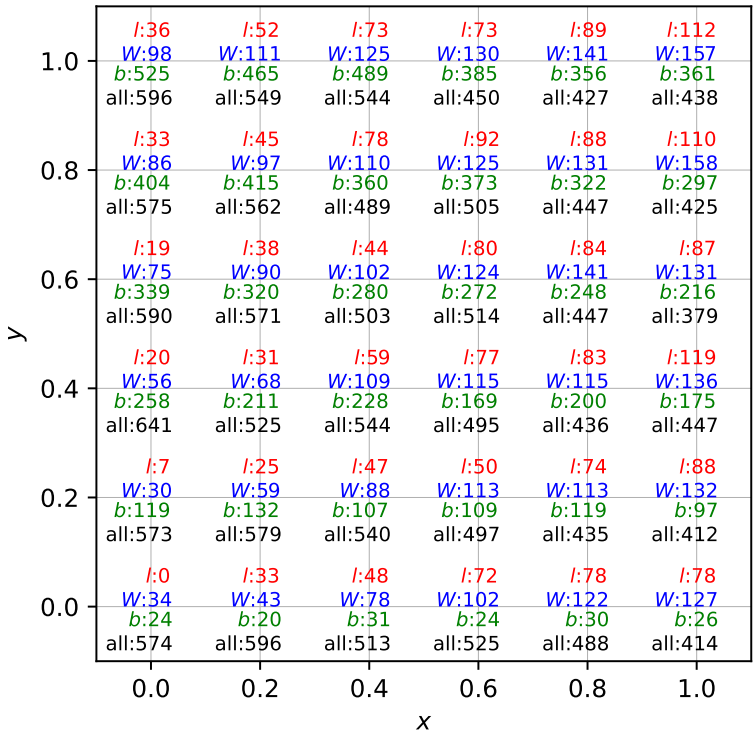

Figure 2: The numbers of events categorized in L1 (red), W1 (blue), and B2 (green), as well as the total number of the signal events (black) for the sample point 1, taking the 100000 events.

In the analysis, we take the reference points with $(x_0, y_0) = (0.5, 0.5)$, $(0.1, 0.9)$, $(0.9, 0.1)$ and $(0.9, 0.9)$. We can see that the analysis of our proposal can give information about the partial branching ratios of the gluino for both sample points 1 and 2. The figures indicate that the accuracy of the y determination is better than that of x. This is because, for the reference points we used, the number of b-tagged jets is larger than that of leptons and boosted W-jets. Note that the expected accuracy of the x determination can be better if more leptons can be used for the analysis. For example, the statistics can be improved by lowering the p_T cut for the leptons. Currently, leptons with $p_T > 200\,\mathrm{GeV}$ are used for the analysis; we have checked that, if the p_T cut for the leptons can be lowered, the sensitivity to the x parameter becomes better. However, low p_T leptons may be produced by the initial state radiations which we do not simulate in our analysis, so we do not pursue this direction.

Now we comment on possible sources of systematic errors that have not been considered so far. The analysis of our proposal relies on the assumption that, once the model parameters (in the present case, x and y, as well as the gaugino masses and the Wino lifetime) are fixed, reliable calculations of the numbers of events in the signal regions can be performed. This

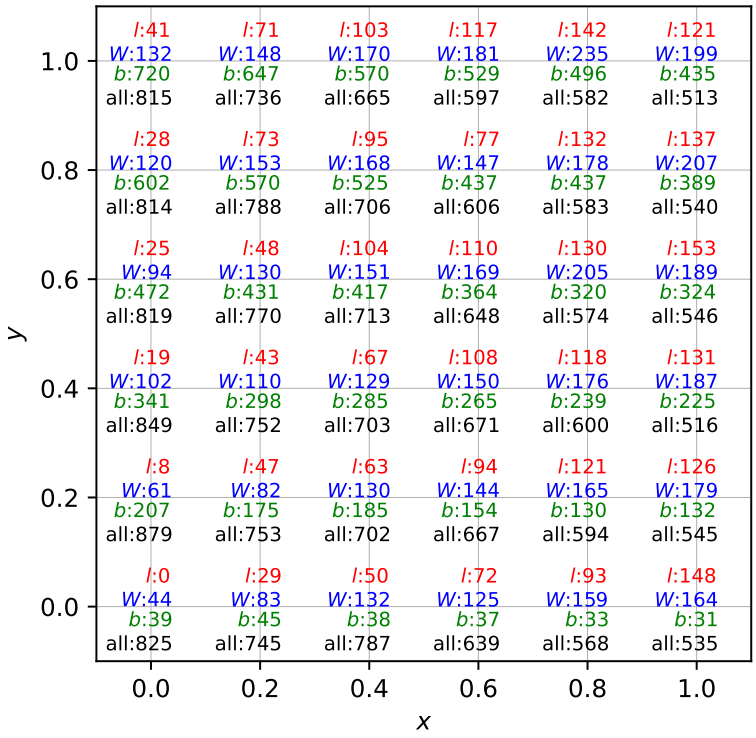

Figure 3: Same as Fig. 2, except for the sample point 2.

may be the case in particular at the time when the FCC-hh experiment will start. The calculations of the numbers of events, however, are likely to be affected by uncertainties in the model, beam, and detector parameters. Here, we perform a simple estimation of the systematic errors by assuming that the systematic uncertainties in the number of events to be of ~ 10 %, for example. (More precise estimation of the uncertainty in the determination of the model parameters x and y is beyond the scope of this paper because it requires a detailed understanding of the sources of systematic errors at the time of the FCC-hh, which is currently quite uncertain.) By varying the number of events in the trial points $N_i^{(x,y)}$ in Eq. (3.11) by ~ 10 % while fixing $N_i^{(x_0,y_0)}$, we found that the changes of the upper and lower bounds on the x are ~ 10 % and are smaller than the error in the x determination shown in Figs. 4 and 5. On the contrary, the uncertainty in the total number of events does not affect so much the y determination because, as indicated in Fig. 2, the number of signal event is insensitive to the y-parameter. One of the sources of the uncertainty is the error in the gluino mass. Analyzing the invariant mass distribution of the decay products of the gluino, the gluino mass can be determined with an accuracy of a few % [10], which results in $\sim 20\%$ uncertainty of the gluino production cross section. The uncertainties due to the luminosity

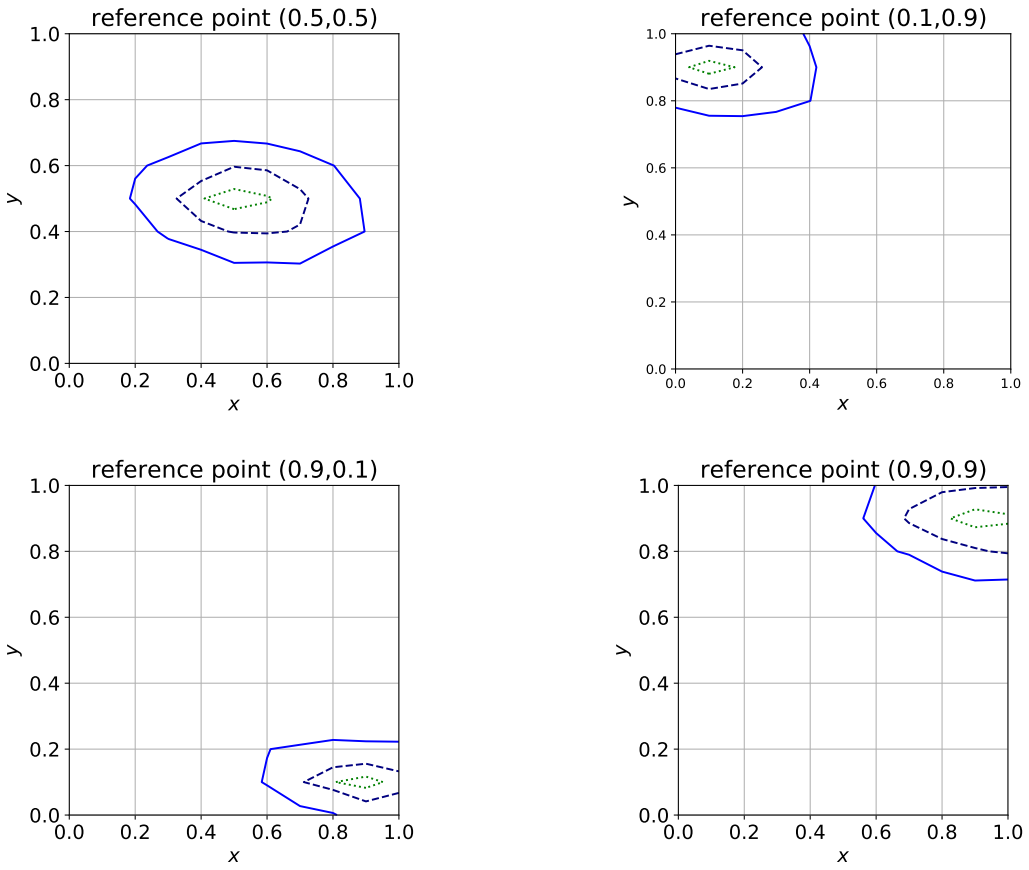

Figure 4: The expected 95 % C.L. constraints on the (x, y) plane for the case of the sample point 1. The reference point is taken to be $(0.5, 0.5)$ (top left), $(0.1, 0.9)$ (top right), $(0.9, 0.1)$ (bottom left), and $(0.9, 0.9)$ (bottom right). The green dotted, navy dashed and blue solid contours are for the integrated luminosity of 10, 3, and 1 ab^{-1}, respectively.

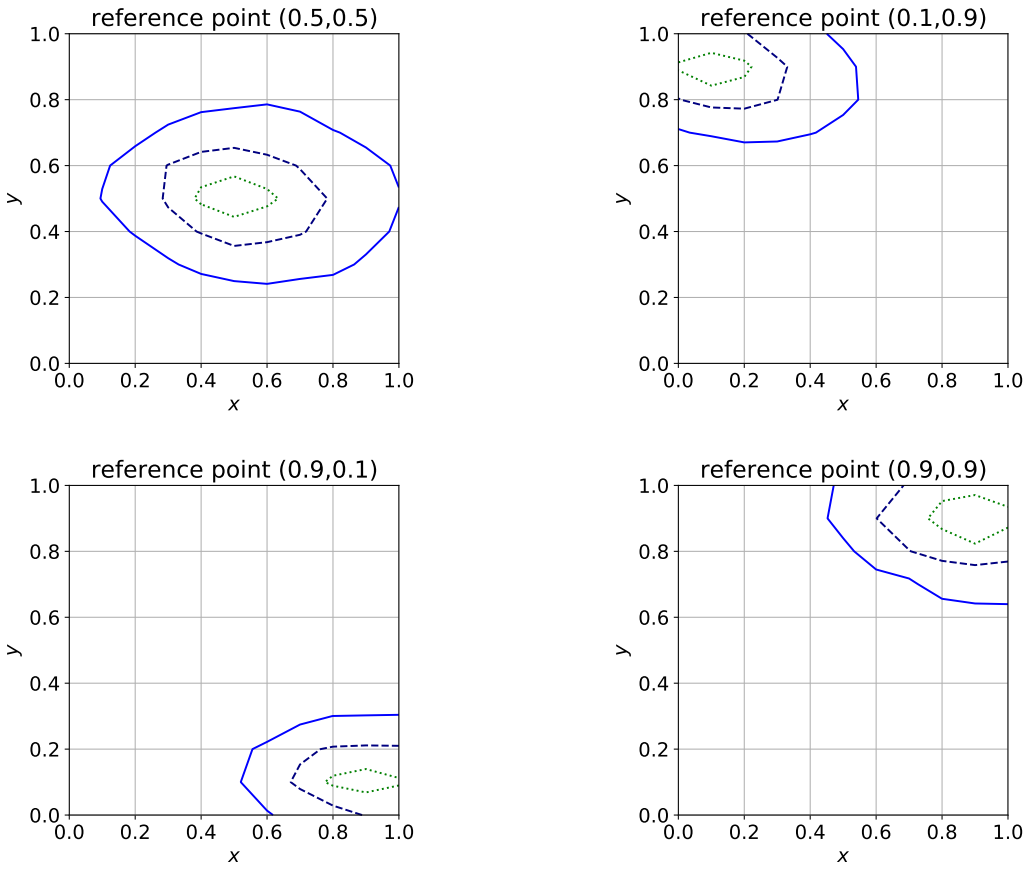

Figure 5: The expected 95 % C.L. constraints on the (x, y) plane for the case of the sample point 2. The reference point is taken to be $(0.5, 0.5)$ (top left), $(0.1, 0.9)$ (top right), $(0.9, 0.1)$ (bottom left), and $(0.9, 0.9)$ (bottom right). The green dotted, navy dashed and blue solid contours are for the integrated luminosity of 10, 3, and $1\,\mathrm{ab}^{-1}$, respectively.

and the parton distribution function may be of the same size. Another possible source of the systematic error is the Wino lifetime. Theoretically the Wino lifetime can be calculated with an accuracy of a few % [22], while the experimental measurement of the Wino lifetime is possible at the FCC-hh with the accuracy of ~ 14 % by using the flight length distribution [11]. We checked that, if the Wino lifetime has an error of $5 - 10$ %, the uncertainty of the total number of events is $\sim 10 - 20$ %. Thus, we expect that the uncertainties in the number of events can be controlled to be $O(10)$ %, and that the systematic errors in the x and y determinations can be smaller than the statistical ones.

4 Implication

So far, we have seen that we can determine the partial branching ratios of the gluino at the FCC-hh with certain accuracies if the gluino is within the kinematical reach. One important implication is that the determination of the partial branching ratios can give us information about the mass spectrum of squarks.

To see this, we perform a simplified analysis. The branching ratios in Eqs. (3.7) – (3.9) are realized when the squark masses have the following relations parameterized by r_R and r_3 (see Eqs. (2.2) – (2.6)):

$$m_{\tilde{d}_i} = \frac{1}{\sqrt{2}} m_{\tilde{u}_i} \equiv r_R m_{\tilde{Q}_i}, \tag{4.1}$$

$$\frac{m_{\tilde{Q}_3}}{m_{\tilde{Q}_{1,2}}} = \frac{m_{\tilde{u}_3}}{m_{\tilde{u}_{1,2}}} = \frac{m_{\tilde{d}_3}}{m_{\tilde{d}_{1,2}}} \equiv r_3. \tag{4.2}$$

Then, the parameters x and y are related to the parameters r_R and r_3 as:

$$x = \frac{\kappa(1 + 4r_R^{-4})}{27 + \kappa(1 + 4r_R^{-4})}, \tag{4.3}$$

with

$$\kappa = \tan^2\theta_W \frac{f(m_{\tilde{B}}/m_{\tilde{g}})}{f(m_{\tilde{W}}/m_{\tilde{g}})}, \tag{4.4}$$

and

$$y = \frac{1}{2r_3^4 + 1}. \tag{4.5}$$

Fig. 6 shows the shapes of r_R and r_3. They are flat when the squark masses are fairly degenerate. Thus, in such a parameter region, the determinations of x and y parameters can provide lower and upper bounds on squark mass ratios. On the contrary, if the squark masses are hierarchical, we can obtain lower or upper bounds on the mass ratios.

In order to see how well the r_R and r_3 parameters are determined, we convert the constraint on the (x, y) plane obtained in the previous section to the constraint on the (r_R, r_3)

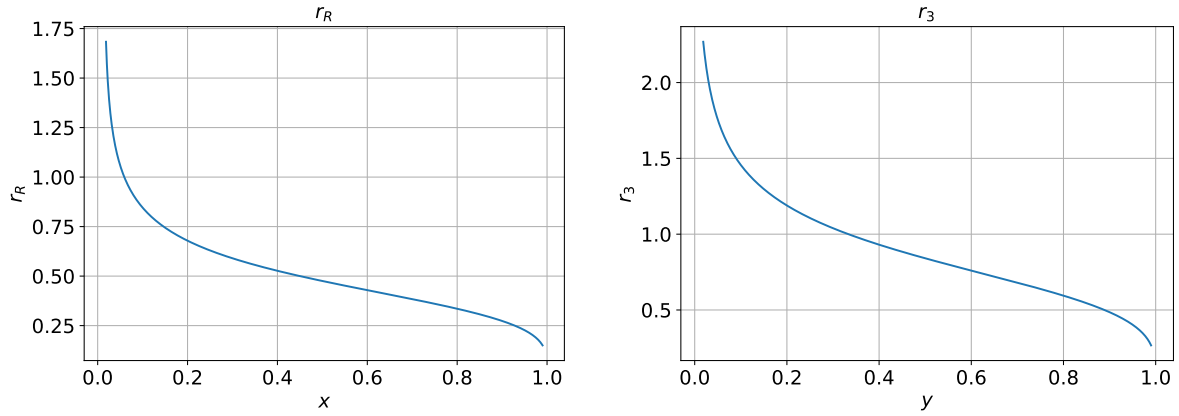

Figure 6: r_R (left) and r_3 (right) as functions of x and y, respectively, for the sample point 1. The behavior of r_R for the sample point 2 looks almost the same.

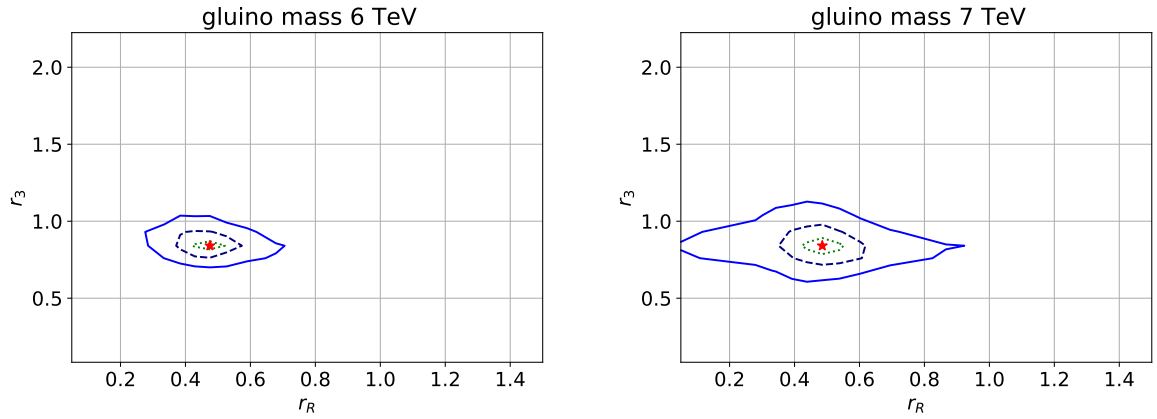

Figure 7: The 95% C.L. constraints on the (r_R, r_3) plane for the sample point 1 (left) and 2 (right). The green dotted, navy dashed, and blue solid contours are for the integrated luminosity of 10, 3, and 1 ab^{-1}, respectively. The reference point corresponds to $(x, y) = (0.5, 0.5)$ and is indicated by the red star on the figure.

plane for the sample points 1 and 2. (The parameter κ is $\kappa \simeq 0.34$ and 0.37, respectively.) Fig. 7 shows the contour of 95% C.L. constraint on the (r_R, r_3) plane, adopting the reference point of $(x_0, y_0) = (0.5, 0.5)$. We can see that, for the reference point with r_3 and r_R being both ~ 1, the analysis of our proposal can determine the mass ratios of squarks.

5 Summary

In this paper, we have discussed the possibility of studying the decay properties of the gluino at future circular pp collider with the center of mass energy of ~ 100 TeV (dubbed as FCC-hh). In the pure gravity mediation model, in which squarks are much heavier than the gauginos, the gluino can decay as $\tilde{g} \to \tilde{W} q \bar{q}'$ and $\tilde{g} \to \tilde{B} q \bar{q}'$. The gaugino in the final state, as well as the flavors of the daughter quarks, are highly model dependent; they depend on the mass spectrum of squarks. We have shown that, with the study of the number of leptons, boosted W-jets, and b-tagged jets, FCC-hh may determine the partial branching ratios of the gluino. We may understand the gaugino species from the decay of the gluino by studying the numbers of leptons and boosted W-jets, while the quark flavors in the final state may be understood by counting the number of b-tagged jets. The decay properties of the gluino are sensitive to the squark masses. We have demonstrated that, with the measurement of the gluino partial branching ratios, FCC-hh can provide information about the squark mass spectrum even if squarks are out of the kinematical reach.

Acknowledgments

This work was supported by JSPS KAKENHI Grant Numbers 20J00046[SC], 19H05810 [KH], 19H05802 [KH], and 20H01897 [KH], 16H06490 [TM], 18K03608 [TM]. SC was supported by the Director, Office of Science, Office of High Energy Physics of the U.S. Department of Energy under the Contract No. DE-AC02-05CH1123.

References

[1] ATLAS collaboration, *Observation of a new particle in the search for the Standard Model Higgs boson with the ATLAS detector at the LHC*, *Phys. Lett. B* **716** (2012) 1 [1207.7214].

[2] CMS collaboration, *Observation of a New Boson at a Mass of 125 GeV with the CMS Experiment at the LHC*, *Phys. Lett. B* **716** (2012) 30 [1207.7235].

[3] M. Saito, R. Sawada, K. Terashi and S. Asai, *Discovery reach for wino and higgsino dark matter with a disappearing track signature at a 100 TeV pp collider*, *Eur. Phys. J. C* **79** (2019) 469 [1901.02987].

[4] T. Golling et al., *Physics at a 100 TeV pp collider: beyond the Standard Model phenomena*, *CERN Yellow Rep.* (2017) 441 [1606.00947].

[5] M. Ibe, T. Moroi and T.T. Yanagida, *Possible Signals of Wino LSP at the Large Hadron Collider*, *Phys. Lett. B* **644** (2007) 355 [hep-ph/0610277].

[6] M. Ibe and T.T. Yanagida, *The Lightest Higgs Boson Mass in Pure Gravity Mediation Model*, *Phys. Lett. B* **709** (2012) 374 [1112.2462].

[7] N. Arkani-Hamed, A. Gupta, D.E. Kaplan, N. Weiner and T. Zorawski, *Simply Unnatural Supersymmetry*, 1212.6971.

[8] L. Randall and R. Sundrum, *Out of this world supersymmetry breaking*, *Nucl. Phys. B* **557** (1999) 79 [hep-th/9810155].

[9] G.F. Giudice, M.A. Luty, H. Murayama and R. Rattazzi, *Gaugino mass without singlets*, *JHEP* **12** (1998) 027 [hep-ph/9810442].

[10] S. Asai, S. Chigusa, T. Kaji, T. Moroi, M. Saito, R. Sawada et al., *Studying gaugino masses in supersymmetric model at future 100 TeV pp collider*, *JHEP* **05** (2019) 179 [1901.10389].

[11] S. Chigusa, Y. Hosomi, T. Moroi and M. Saito, *Determining Wino Lifetime in Supersymmetric Model at Future 100 TeV pp Colliders*, *Phys. Lett. B* **803** (2020) 135260 [1912.00592].

[12] R. Sato, S. Shirai and K. Tobioka, *Gluino Decay as a Probe of High Scale Supersymmetry Breaking*, *JHEP* **11** (2012) 041 [1207.3608].

[13] R. Sato, S. Shirai and K. Tobioka, *Flavor of Gluino Decay in High-Scale Supersymmetry*, *JHEP* **10** (2013) 157 [1307.7144].

[14] Particle Data Group collaboration, *Review of Particle Physics*, *PTEP* **2020** (2020) 083C01.

[15] Y. Okada, M. Yamaguchi and T. Yanagida, *Upper bound of the lightest Higgs boson mass in the minimal supersymmetric standard model*, *Prog. Theor. Phys.* **85** (1991) 1.

[16] J.R. Ellis, G. Ridolfi and F. Zwirner, *Radiative corrections to the masses of supersymmetric Higgs bosons*, *Phys. Lett. B* **257** (1991) 83.

[17] H.E. Haber and R. Hempfling, *Can the mass of the lightest Higgs boson of the minimal supersymmetric model be larger than m(Z)?*, *Phys. Rev. Lett.* **66** (1991) 1815.

[18] T. Moroi and M. Nagai, *Probing Supersymmetric Model with Heavy Sfermions Using Leptonic Flavor and CP Violations*, *Phys. Lett. B* **723** (2013) 107 [1303.0668].

[19] D. McKeen, M. Pospelov and A. Ritz, *Electric dipole moment signatures of PeV-scale superpartners*, *Phys. Rev. D* **87** (2013) 113002 [1303.1172].

[20] J. Hisano, S. Matsumoto, M. Nagai, O. Saito and M. Senami, *Non-perturbative effect on thermal relic abundance of dark matter*, *Phys. Lett. B* **646** (2007) 34 [hep-ph/0610249].

[21] C. Borschensky, M. Krämer, A. Kulesza, M. Mangano, S. Padhi, T. Plehn et al., *Squark and gluino production cross sections in pp collisions at $\sqrt{s}$ = 13, 14, 33 and 100 TeV*, *Eur. Phys. J. C* **74** (2014) 3174 [1407.5066].

[22] M. Ibe, S. Matsumoto and R. Sato, *Mass Splitting between Charged and Neutral Winos at Two-Loop Level*, *Phys. Lett. B* **721** (2013) 252 [1212.5989].

[23] R. Barbieri, G. Gamberini, G.F. Giudice and G. Ridolfi, *Constraining supergravity models from gluino production*, *Nuclear Physics B* **301** (1988) 15 .

[24] P. Gambino, G. Giudice and P. Slavich, *Gluino decays in split supersymmetry*, *Nucl. Phys. B* **726** (2005) 35 [hep-ph/0506214].

[25] J. Thaler and K. Van Tilburg, *Identifying Boosted Objects with N-subjettiness*, *JHEP* **03** (2011) 015 [1011.2268].

[26] CMS collaboration, *Identification techniques for highly boosted W bosons that decay into hadrons*, *JHEP* **12** (2014) 017 [1410.4227].

[27] J. Alwall, M. Herquet, F. Maltoni, O. Mattelaer and T. Stelzer, *MadGraph 5 : Going Beyond*, *JHEP* **06** (2011) 128 [1106.0522].

[28] J. Alwall, R. Frederix, S. Frixione, V. Hirschi, F. Maltoni, O. Mattelaer et al., *The automated computation of tree-level and next-to-leading order differential cross sections, and their matching to parton shower simulations*, *JHEP* **07** (2014) 079 [1405.0301].

[29] T. Sjöstrand, S. Ask, J.R. Christiansen, R. Corke, N. Desai, P. Ilten et al., *An introduction to PYTHIA 8.2*, *Comput. Phys. Commun.* **191** (2015) 159 [1410.3012].

[30] DELPHES 3 collaboration, *DELPHES 3, A modular framework for fast simulation of a generic collider experiment*, *JHEP* **02** (2014) 057 [1307.6346].

[31] A.D. Martin, W.J. Stirling, R.S. Thorne and G. Watt, *Parton distributions for the LHC*, *Eur. Phys. J. C* **63** (2009) 189 [0901.0002].

[32] R. Brun and F. Rademakers, *ROOT: An object oriented data analysis framework*, *Nucl. Instrum. Meth. A* **389** (1997) 81.